HABITAT FRAGMENTATION

Fragmentation increased in over half of global forests from 2000 to 2020

Yibiao Zou[1]*, Thomas W. Crowther[1,2], Gabriel Reuben Smith[1], Haozhi Ma[3], Lidong Mo[1,4], Lalasia Bialic-Murphy[1], Peter Potapov[5,6], Klementyna A. Gawecka[7,8], Chi Xu[9], Pablo J. Negret[10,11], Thomas Lauber[1], Zhaofei Wu[1,3,12], Dominic Rebindaine[1], Constantin M. Zohner[1]

Habitat fragmentation, in which contiguous forests are broken into smaller, isolated patches, threatens biodiversity by disrupting species movement, shrinking populations, and altering ecosystem dynamics. Past assessments suggested declining global fragmentation, but they relied on structure-based metrics that overlook ecological connectivity. We analyzed global forest fragmentation from 2000 to 2020 using complementary metrics that captured patch connectivity, aggregation, and structure. Connectivity-based metrics revealed that 51 to 67% of forests globally—and 58 to 80% of tropical forests—became more fragmented, which is nearly twice the rate suggested by traditional structure-focused methods (30 to 35%). Aggregation-focused metrics confirmed increases in 57 to 83% of forests. Human activities such as agriculture and logging drive this change. Yet protected tropical areas saw up to an 82% reduction in fragmentation, underscoring the potential of targeted conservation.

Forests are essential to global biodiversity and climate regulation (*1*–*6*). Yet human activities increasingly threaten them, not only by reducing forest area but also by fragmenting forests into smaller, isolated patches (*7*–*10*). This process, known as habitat fragmentation (hereafter "fragmentation"), reduces species richness and carbon storage (*11*–*13*). Its importance, particularly regarding ecological connectivity and integrity, is emphasized in global policy frameworks such as the Aichi Target 11 and the Kunming-Montreal Global Biodiversity Framework (*14*, *15*). Accurately quantifying fragmentation is critical not only to understand its global extent but also to identify high-risk regions and guide conservation efforts.

Fragmentation arises through multiple pathways: Patches may shrink, split, vanish, stretch into complex shapes, or grow more distant (Fig. 1, A to E). These changes often co-occur, as in ongoing Amazon deforestation (Fig. 1F and fig. S2), and affect biodiversity through three main mechanisms (*16*–*21*). First, new edges change microclimates and disturbance regimes, often making forests warmer and drier (*22*, *23*). Second, shrinking core areas threaten species that are dependent on large, intact habitats (*11*). Third, increased patch isolation disrupts connectivity and reduces movement, often leading to long-term population declines (*24*–*26*). Although edge effects vary, losses of core habitat and connectivity consistently harm forest specialists (*11*, *17*).

To assess these impacts, researchers use a range of landscape metrics (*27*–*32*), broadly categorized into structure, aggregation, and connectivity (*7*, *11*). Structure-focused metrics quantify habitat subdivision—including patch number, size, and edge length—but often neglect the habitat extent and spatial arrangement (*7*). Aggregation-focused metrics assess how clustered patches are but may also overlook overall extent. Connectivity-focused metrics incorporate both patch area and spatial configuration, offering a more ecologically relevant perspective. Because each captures different aspects of fragmentation, selecting ecologically meaningful metrics is critical to accurately track progress toward conservation goals (*27*, *33*).

Connectivity- and aggregation-focused studies suggest that fragmentation has increased in recent decades, particularly in the tropics (*34*–*36*). For example, Hansen *et al.* found consistent tropical forest patch loss from 2001 to 2018, with smaller patches disappearing fastest (*35*). Edge habitat also expanded from 2000 to 2010, increasing exposure to disturbances (*36*). However, global assessments that used structure-focused metrics reported declining fragmentation in 75% of forests from 2000 to 2020 (*7*) despite a net forest loss of 101 Mha (*37*). This discrepancy arises because structure metrics define fragmentation by patch number and size, interpreting fewer, larger patches as reduced fragmentation (Fig. 1, C and F), even when ecologically critical patches are lost (*7*, *33*, *38*, *39*). Such losses reduce connectivity and harm species that depend on stepping-stone habitats for dispersal and persistence (*11*, *13*, *19*).

In conservation biology, debate persists over whether habitat configuration (Fig. 1A) or total area plays a greater role in shaping biodiversity (*13*, *17*–*19*). Structure-focused metrics are valuable for isolating the effects of fragmentation per se—that is, changes in patch structure without habitat loss (*11*, *19*). However, they often overlook critical aspects such as connectivity and aggregation, which limits their ability to capture how landscape change affects species movement, resource access, and population viability (*7*, *11*, *13*). As such, they can misrepresent fragmentation trends over time. A comprehensive global assessment must therefore integrate connectivity- and aggregation-focused metrics to fully reflect fragmentation's ecological impacts and its drivers.

We quantified global forest fragmentation from 2000 to 2020 using a comprehensive set of metrics that represent habitat connectivity, aggregation, and structure (Table 1, Fig. 1, and fig. S1). We calculated nine widely used fragmentation metrics (*7*, *27*–*30*, *32*), grouped into three categories on the basis of their ecological focus. Connectivity metrics included total core forest area (TCA), largest patch index (LPI), and landscape division index [LDI; probability that two randomly placed individuals occur in the same forest patch (*29*)]. Aggregation metrics included aggregation index (AI), percentage of like adjacency (PLADJ), and mean Euclidean nearest-neighbor distance among patches (ENN). Structural metrics included mean patch area (MPA), edge density (ED), and number of patches (NP) (detailed descriptions are provided in Table 1 and table S1). To capture broader fragmentation trends, we synthesized these into three composite indices: the connectivity-based fragmentation index (CFI), the aggregation-based fragmentation index (AFI) (*27*–*30*, *32*), and the structure-based fragmentation index [SFI, formerly termed the forest fragmentation index (FFI) in Ma *et al.* (*7*)]. We first established how each metric responds to hypothetical and real-world landscape changes, demonstrating their ecological relevance. We then applied them to high-resolution (30 m) global forest cover data (*37*) to map trends in fragmentation, identify key drivers (*8*), and evaluate the effectiveness of protected areas in mitigating fragmentation.

[1]Institute of Integrative Biology, ETH Zurich (Swiss Federal Institute of Technology), Zurich, Switzerland. [2]Oath, The Presidio of San Francisco, San Francisco, CA, USA. [3]Swiss Federal Institute for Forest, Snow and Landscape Research WSL, Birmensdorf, Switzerland. [4]Department of Plant Biology and Ecology, College of Life Sciences, Nankai University, Tianjin, China. [5]World Resources Institute, Washington, DC, USA. [6]Department of Geographical Sciences, University of Maryland, College Park, MD, USA. [7]Department of Evolutionary Biology and Environmental Studies, University of Zurich, Zurich, Switzerland. [8]UK Centre for Ecology and Hydrology, Bush Estate, Penicuik, UK. [9]School of Life Sciences, Nanjing University, Nanjing, China. [10]Wyss Academy for Nature, Centre for Development and the Environment, Institute of Geography, University of Bern, Bern, Switzerland. [11]Hawkesbury Institute for the Environment, Western Sydney University, Richmond, Australia. [12]College of Water Sciences, Beijing Normal University, Beijing, China. ***Corresponding author.** **Email: yibiao.zou@usys.ethz.ch**

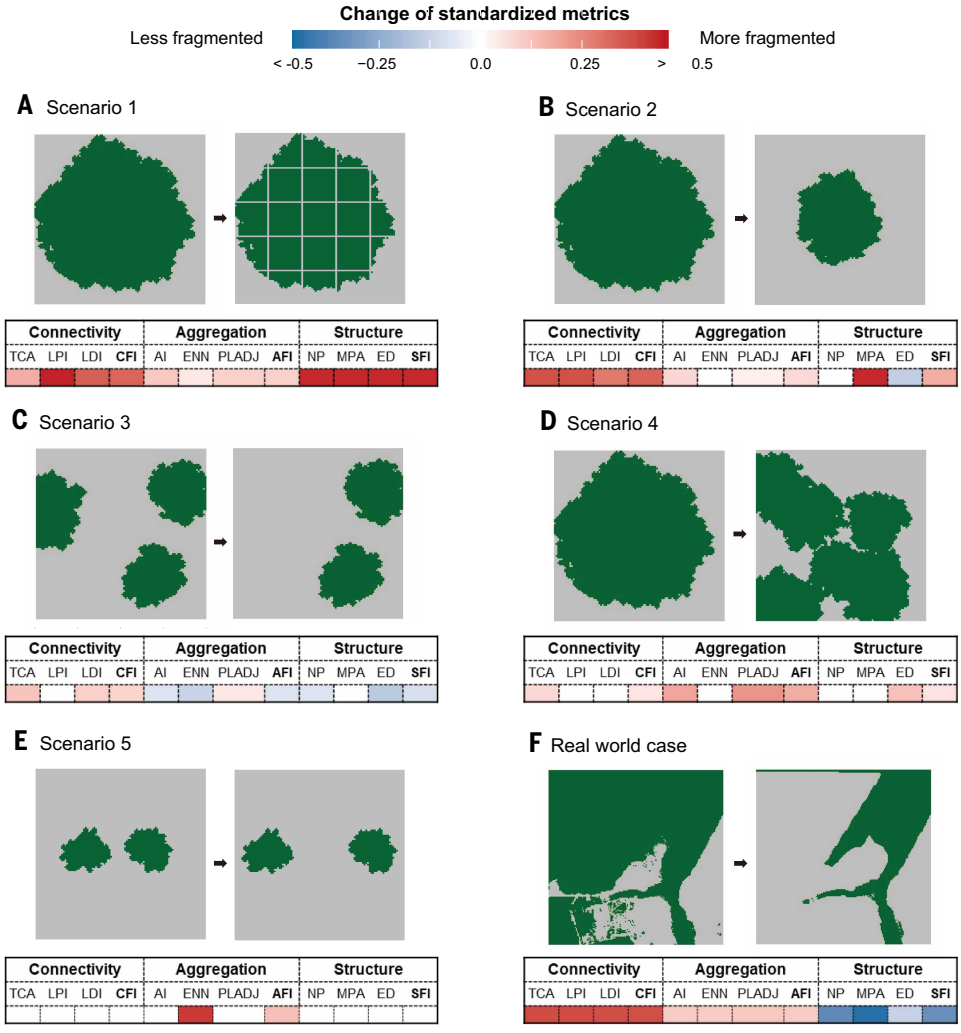

Fig. 1. Responses of fragmentation metrics to simulated and observed landscape change scenarios. (**A**) Transition from a single forest patch with 60% canopy cover to multiple smaller patches with minimal cover loss. (**B**) Reduction of a single forest patch from 60 to 20% cover. (**C**) Removal of one of three equally sized forest patches. (**D**) Transformation of a circular patch with 60% cover into an irregular shape with the same coverage but a longer perimeter. (**E**) Increased distance between two previously proximate patches. (**F**) Observed deforestation in an Amazon forest site from (left) 2000 (72% cover) to (right) 2020 (26% cover). Similar patterns occur in other sites (fig. S2). Our analysis shows that scenarios 2 and 3 are the most prevalent globally, affecting 18 and 46% of forests experiencing cover loss, respectively (fig. S3). Although scenarios 4 and 5 are hypothetical and may not frequently occur in real forested landscapes, they help to illustrate how aggregation-focused metrics respond to changes in patch shape and distance compared with connectivity- and structure-focused metrics. For each scenario, changes were assessed by using 12 normalized fragmentation metrics (scaled from 0 to 1) (Table 1 and table S1), categorized into three groups: connectivity-focused, aggregation-focused, and structure-focused metrics. Positive values indicate increased fragmentation. Red indicates a fragmentation increase, blue indicates a decrease, and white indicates no change, with darker shades representing greater magnitude. The CFI, AFI, and SFI, which represent integrated indices for connectivity, aggregation, and structure, are highlighted in bold.

Results

Fragmentation metrics respond differently to landscape change

Fragmentation metrics responded differently depending on the type of landscape alteration (Fig. 1). All metric groups detected increased fragmentation when forest patches were subdivided without substantial forest loss, with structure-focused metrics showing the strongest response to patch division (Fig. 1A). By contrast, connectivity-focused metrics consistently indicated increased fragmentation in scenarios that involved shrinking patches (Fig. 1B), the disappearance of patches (Fig. 1C), and real-world deforestation (Fig. 1F). In these cases, structure-focused metrics often suggested reduced fragmentation, highlighting their insensitivity to losses in habitat connectivity. Aggregation-focused metrics were especially responsive to increases in patch shape complexity (Fig. 1D) and patch distance (Fig. 1E) but indicated reduced fragmentation when patches disappeared (Fig. 1C), resulting in variable outcomes in real-world scenarios (Fig. 1F and fig. S2). Only the aggregation-focused ENN and the composite AFI detected increased fragmentation when patch separation increased without loss of area (Fig. 1E), underscoring their particular sensitivity to spatial configuration.

To quantify how these fragmentation dimensions manifest globally, we conducted a principal components analysis (PCA) on all individual and composite metrics. We also incorporated metapopulation capacity (MPC)—a measure of functional connectivity that reflects a landscape's ability to support species persistence (*25*, *31*). The PCA biplot revealed three statistically distinct metric clusters [multivariate analysis of variance (MANOVA) P value < 0.001], corresponding to habitat connectivity, aggregation, and structure (Fig. 2A). Connectivity-focused metrics aligned closely with MPC, confirming their strength in capturing functional connectivity and ecologically meaningful fragmentation (Fig. 2A and fig. S10C). This underscores the importance of incorporating connectivity-based approaches in global fragmentation assessments to better understand biodiversity impacts and conservation priorities.

Trends of global fragmentation from 2000 to 2020

To quantify global forest fragmentation trends, we assessed the proportion of forest area that showed increased fragmentation from 2000 to 2020 at multiple spatial resolutions (5, 10, 20, and 40 km). We used three composite indices—CFI, AFI, and SFI—to capture trends globally and across major forest biomes (tropical, temperate, and boreal). The results reveal stark differences among metric types. The CFI indicates that depending on grid size, 51 to 67% of forests globally (Fig. 2C), and 58 to 80% of tropical forests (Fig. 2D), have become more fragmented. Similarly, the AFI suggests that 57 to 83% of global forests became more fragmented, reflecting declines in spatial proximity and ecological connectivity, both of which are crucial for species movement and habitat continuity. By contrast, the SFI suggests that only 30 to 35% of forests worldwide became more fragmented over the same period (Fig. 2C), which aligns with earlier findings (*7*). This discrepancy arises because the SFI interprets the loss of small or connecting patches as reduced fragmentation because of SFI's focus on patch number and size rather than ecological connectivity.

Table 1. Overview of landscape-level fragmentation metrics.

	Metric	Full name	Description	Reference
	Canopy cover	Forest cover percentage	The percentage of the landscape covered by forests	McGarigal *et al*. (*27*)
Connectivity-focused	TCA	Total core area	The sum of core areas of all patches belonging to forests. A cell is defined as core area if all of its neighboring cells are forests.	McGarigal *et al*. (*27*)
	LPI	Largest patch index	The percentage of the landscape covered by the corresponding largest patch of forest	McGarigal *et al*. (*27*)
	LDI	Landscape division index	The probability that two randomly selected cells are not located in the same patch of forest	Jaeger (*29*)
	CFI	Connectivity-based fragmentation index	Synthetic metric integrating TCA, LPI, and LDI	This paper
Aggregation-focused	AI	Aggregation index	The number of like adjacencies divided by the theoretical maximum possible number of like adjacencies for forest cells	He *et al*. (*30*)
	PLADJ	Percentage of like adjacency	The number of adjacencies between forest cells divided by the number of adjacencies between forest and nonforest cells	McGarigal *et al*. (*27*)
	ENN	Mean of Euclidean nearest-neighbor distance	The mean Euclidean distance to the nearest neighboring patch for each forest patch	McGarigal *et al*. (*27*)
	AFI	Aggregation-based fragmentation index	Synthetic metric integrating AI, PLADJ, and ENN	This paper
Structure-focused	NP	Number of patches	Number of distinct forest patches	McGarigal *et al*. (*27*)
	MPA	Mean patch area	The mean of all patch areas belonging to forests	McGarigal *et al*. (*27*)
	ED	Edge density	The length sum of all edges of forest divided by the landscape area (in our study, the landscape area is the grid cell area)	McGarigal *et al*. (*27*)
	SFI	Structure-based fragmentation index	Synthetic metric integrating NP, MPA, and ED. This index was called FFI in Ma *et al*. (*7*).	Ma *et al*. (*7*)
Functional connectivity	MPC	Metapopulation capacity	A relative measure of the ability of a spatially explicit landscape to support long-term species persistence based on connectivity and area of habitat	Hanski and Ovaskainen (*31*)

Fragmentation estimates from the CFI and AFI were scale-dependent, with higher fragmentation detected at coarser resolutions (10 to 40 km) (Fig. 2, C and D). This reflects the edge-driven nature of fragmentation: As grid size increases, fewer cells fall within intact cores, increasing the apparent fragmentation rate. By contrast, the SFI remained largely scale-insensitive, even indicating slight declines in fragmentation at larger scales (Fig. 2, C and D).

To examine how fragmentation metrics respond to deforestation, we related each composite metric to forest cover at a 5-km resolution for the years 2000 (Fig. 2B) and 2020 (fig. S5). CFI and AFI values declined with increasing forest cover, aligning with ecological expectations that larger, contiguous forests are less fragmented (*11*). By contrast, the SFI indicated reduced fragmentation in areas with both low and high forest cover, thus equating severe deforestation with reduced fragmentation and highlighting its limitations in capturing deforestation-driven fragmentation. Spatial analysis confirms that these discrepancies between metrics are most pronounced across the pantropical regions (fig. S9), where deforestation is severe (*8*, *35*).

Drivers of forest fragmentation

Forest fragmentation and cover loss arise from various processes that can be broadly classified into permanent conversion and temporary disturbances (*8*). Permanent conversion includes commodity-driven deforestation (such as mining and energy development) and urban expansion, resulting in lasting land-use change. Temporary disturbances such as shifting agriculture (agricultural conversion followed by abandonment), forestry (clearcutting or selective logging), and wildfires often allow for forest regrowth over time.

To quantify the contribution of these drivers, we integrated data from the Global Forest Watch dataset (*8*), which maps primary deforestation drivers from 2000 to 2023 (Fig. 3). Results were consistent with earlier assessments (*8*) from 2000 to 2015 (figs. S12 and S13), confirming the growing influence of anthropogenic disturbance, especially shifting agriculture, commodity-driven deforestation, and forestry. We used the CFI at 5-km resolution, the finest available for this analysis and the subsequent assessment of protected areas because it best aligned with ecological indicators of fragmentation (Fig. 2, A and B, and fig. S10).

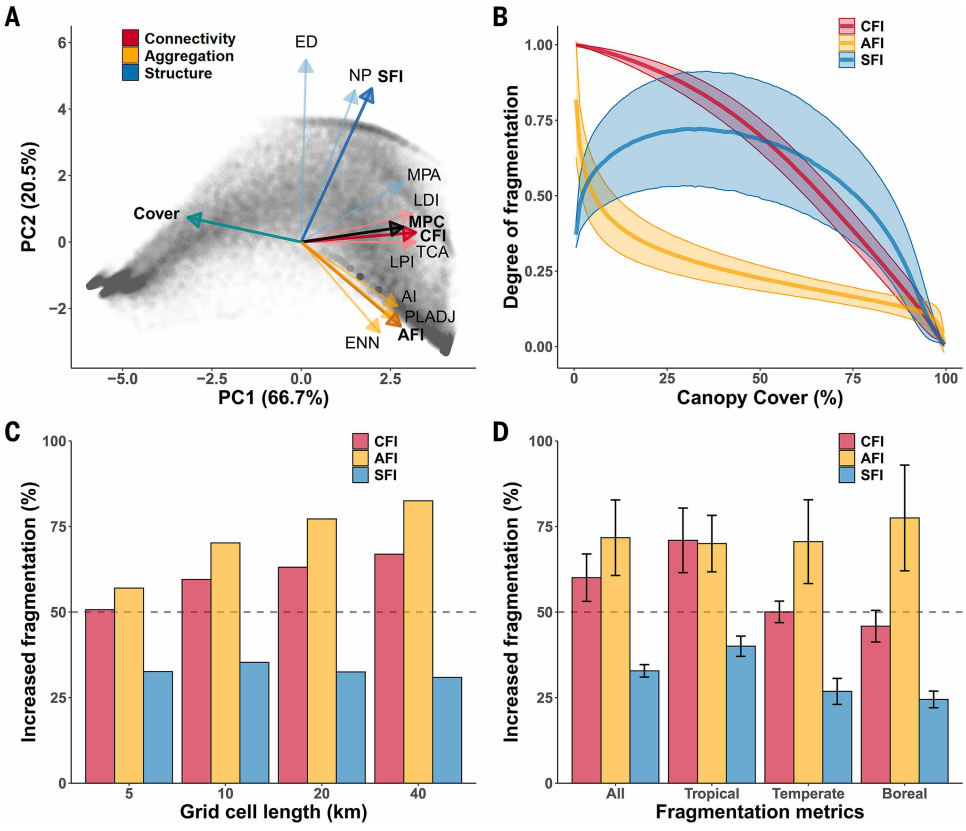

Fig. 2. Classification and analysis of fragmentation metrics. (**A**) Major axes of forest fragmentation: PCA biplot showing the distribution of various fragmentation metrics applied to a 10% random sample of all grid cells (forest cover > 0) for the year 2000. Metrics are color-coded according to their focus: connectivity-focused in red, aggregation-focused in orange, and structure-focused in blue. The integrated indices—CFI, AFI, and SFI [formerly termed FFI from Ma *et al*. (*7*)]—are highlighted in darker shades within their groups. Forest cover (dark cyan) is also included. A pairwise MANOVA confirms significant differences among loadings of these three groups ($P < 0.001$), indicating distinct clustering. The MPC (black), a critical metric for functional connectivity, aligns closely with connectivity-focused metrics. PCA biplots on the 12 fragmentation metrics across all grid cells in both years 2000 and 2020 are provided in fig. S3. (**B**) Relationship between the observed fragmentation degree (based on the CFI, AFI, and SFI) and canopy cover for all analyzed forest grid cells in the year 2000. Solid lines indicate mean fragmentation values; the shaded areas indicate mean ± SD. (**C**) Proportion of global forest grid cell areas with increased fragmentation between 2000 and 2020 at different grid cell scales, based on the CFI, AFI, and SFI. (**D**) Proportion of forest grid cell areas with increased fragmentation (mean ± SD, over different grid cell scales) between 2000 and 2020 across global forest grid cells and in different forest biomes, based on the CFI, AFI, and SFI. (C) and (D) include only forest grid cells with forest cover >30% in 2000. Results remained consistent across different forest cover thresholds used to define forest grid cells (fig. S17).

Globally, shifting agriculture (37% of grids with increased fragmentation) and forestry (34%) were the dominant drivers of increased fragmentation (Fig. 3), followed by wildfires and commodity-driven deforestation (both 14%). In the tropics, fragmentation was overwhelmingly driven by shifting agriculture (61%), whereas temperate forests were mainly affected by forestry (81%). In boreal regions, wildfires (62%) and forestry (38%) were the primary drivers. Permanent conversions from commodity-driven deforestation and urbanization accounted for <15% of fragmentation globally. Identifying these region-specific drivers is essential for designing targeted and effective conservation strategies.

Fragmentation status within and outside protected areas

To examine how protection status influences forest fragmentation, we integrated data from the World Database on Protected Areas (*40*). Area-based protection remains a cornerstone of biodiversity conservation (*41*, *42*), and previous studies have suggested that protected tropical forests face fewer human disturbances (*43*). However, whether this translates into reduced fragmentation rates over time remains unclear.

We classified 5-km forest grid cells into protected and nonprotected categories and applied a matching approach to control for environmental and socioeconomic differences (figs. S14 to S16) (*42*, *44*–*46*). Fragmentation trends from 2000 to 2020 were analyzed across four categories: strictly protected, protected, matched nonprotected, and all nonprotected. Given distinct fragmentation drivers, tropical and nontropical forests were analyzed separately.

In the tropics, fragmentation increased in all categories but remained significantly lower in protected areas. Strictly protected areas experienced 82% less fragmentation than matched nonprotected areas, whereas less strictly protected areas saw a 45% reduction (Fig. 4A). These patterns align with reduced human activity: Shifting agriculture was 59 and 16% lower in strictly and less strictly protected areas, respectively, whereas forestry was 10 and 58% lower (Fig. 4B). These results highlight the effectiveness and importance of tropical protected areas in limiting human-driven fragmentation and underscore the urgent need to expand protection across tropical regions in line with international conservation targets, including Aichi Target 11 and the "30x30" goal of the Kunming-Montreal Global Biodiversity Framework (*14*, *15*).

By contrast, nontropical forests showed slightly higher fragmentation in strictly protected areas compared with nonprotected ones (Fig. 4C), alongside a 63% increase in forestry activity (Fig. 4D). This may reflect inconsistencies in how protection status is defined across jurisdictions, with some areas that allow logging still classified as strictly protected (*43*, *47*).

Discussion

A recent study that used structure-focused metrics suggested that 75% of the world's forests are becoming less fragmented as patch counts decline with forest loss (Fig. 1F) (*7*). Although this conclusion is mathematically valid, our analysis incorporating connectivity and aggregation reveals the opposite: Most forests, especially in the tropics, have become more fragmented over the past two decades. These findings align with prior studies that have shown increasing fragmentation in the tropics, with declining cover, more edge habitats, and reduced core areas (*34*–*36*). This trend holds across varying forest cover thresholds that are used to define forest grid cells (fig. S17) and is primarily driven by declining connectivity and aggregation.

The divergences among fragmentation metrics highlight the importance of assessing not only forest areas but also the spatial arrangement of patches to evaluate changes in landscape integrity (*11*, *12*). Structure-focused metrics, such as the SFI, capture a distinct and

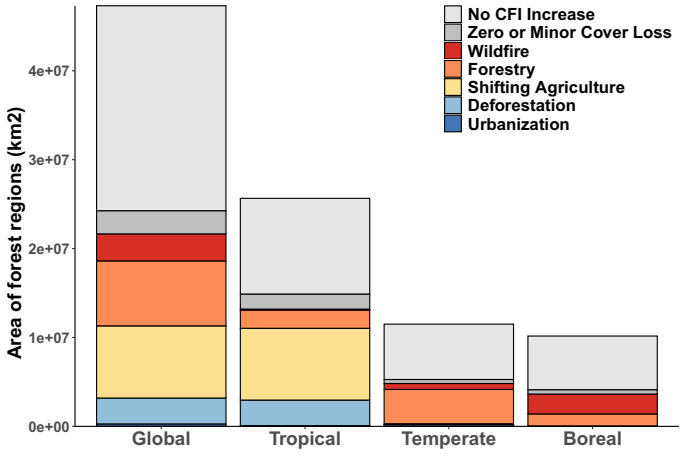

Fig. 3. Drivers of forest fragmentation trends (2000 to 2020) across biomes. Total area of forest regions [grid cells with >30% canopy cover at 2.5 arc min (~5 km) resolution, the finest resolution available] affected by different fragmentation drivers at global and biome scales. "No CFI increase" represents forest regions where fragmentation levels have remained stable or decreased. "Zero or minor cover loss" includes areas where fragmentation slightly increased because of an unknown cause but with minor or no forest cover loss. All other categories represent regions with increased fragmentation driven by specific factors, including (i) "Wildfire," where forest burning occurred without subsequent human conversion or agricultural activity; (ii) "Forestry," representing large-scale harvesting within managed forests with signs of regrowth; (iii) "Shifting agriculture," referring to small- to medium-scale forest conversion for agriculture, later abandoned and followed by forest regrowth; (iv) "Deforestation," characterized by permanent forest loss due to commodity-driven activities such as agriculture, mining, or energy infrastructure; and (v) "Urbanization," where forests have been converted for urban expansion. The drivers are arranged from (top) Wildfire to (bottom) Urbanization to reflect the increasing degree of irreversible forest loss.

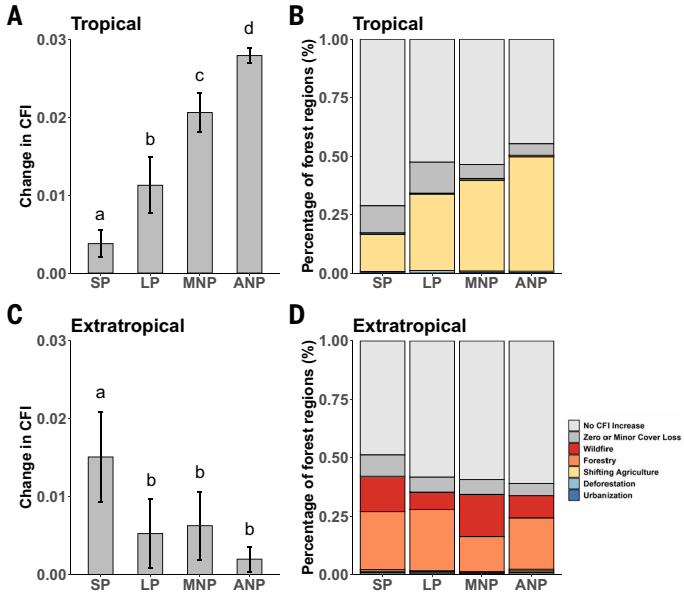

Fig. 4. Forest fragmentation trends (2000 to 2020) inside and outside protected areas. (**A** and **C**) Changes in the degree of fragmentation (indicated with the CFI, mean ± 3 SE) across forest grid cells [at 2.5 arc min (~5 km) resolution] in strictly protected areas (SP), less strictly protected areas (LP), matched nonprotected areas (MNP), and all nonprotected areas (ANP) in (A) tropical and (C) extratropical forests. Kruskal-Wallis and post hoc Mann-Whitney *U* tests (tables S4 and S5) show that (A) in tropical forests, fragmentation levels significantly differ across all protection categories ($P < 0.001$), whereas (C) in extratropical forests, only the "strictly protected" group is significantly different from all other groups ($P < 0.05$). (**B** and **D**) Proportions of forest regions experiencing fragmentation owing to different drivers across different protection categories in (B) tropical and (D) extratropical regions. "No CFI increase" represents areas where fragmentation levels have remained stable or decreased. "Zero or minor cover loss" includes areas where fragmentation slightly increased because of an unknown cause but with minor or no forest cover loss. All other categories represent regions with increased fragmentation driven by specific factors such as forestry, shifting agriculture, deforestation, or urbanization. To address spatial autocorrelation, we only included forest grid cells at least 40 km apart.

meaningful dimension of fragmentation related to patch size, number, and edge complexity (Fig. 2A). They are especially valuable for isolating fragmentation per se from habitat loss (*11*, *17*–*19*) and for comparing sites with similar forest cover but differing patch structures (*13*). However, they reflect only one of three critical axes—structure, aggregation, and connectivity (Fig. 2A)—and can yield misleading results when forest cover changes alongside fragmentation, whether over time or across space. For example, they may indicate reduced fragmentation when patch numbers decline, even as habitat loss degrades connectivity and ecosystem function (Fig. 1C).

By contrast, connectivity- and aggregation-focused metrics offer a more ecologically meaningful perspective for detecting and interpreting fragmentation over time. They show stronger alignment with key ecological indicators such as MPC and net primary productivity (fig. S10) and directly reflect functional landscape properties that affect biodiversity persistence (*25*, *31*). The strong correlation between the CFI and MPC suggests that the CFI offers a computationally efficient proxy for ecological connectivity.

These differences among fragmentation metrics underscore the need for ecologically meaningful indicators in conservation planning (*11*, *19*). For example, both the CFI and AFI detect increased fragmentation across pantropical regions, which is consistent with high deforestation rates (*42*), and reveal 82 and 79% less fragmentation in strictly protected areas compared with matched nonprotected ones, respectively (Fig. 4A and fig. S18). These reductions were largely driven by declines in agricultural activity (Fig. 4B). By contrast, the SFI suggests declining fragmentation both within and outside tropical protected areas (fig. S18), illustrating how reliance on structure-based metrics alone can obscure ecological degradation and potentially mislead conservation efforts. To fully evaluate forest fragmentation and its ecological consequences, all three dimensions—structure, aggregation, and connectivity—must be considered in tandem. However, metrics that capture connectivity and aggregation offer greater ecological relevance for understanding functional landscape change and guiding effective conservation.

Given the ecological relevance of connectivity-focused metrics, we used the CFI to assess the primary drivers of fragmentation and the effectiveness of protected areas across forest biomes. Our analysis shows that permanent forest conversion accounts for only 15% of global connectivity-focused fragmentation, and wildfires—intensified by climate change—contribute another 14% (Fig. 3). The remaining 71% was primarily driven by agricultural and forestry activities that can often represent temporary transitions, highlighting opportunities for restoration (*3*, *8*). Protected areas mitigate these impacts, although their effectiveness varies by biome. Tropical forests benefit most, with reduced fragmentation primarily because of lower agricultural encroachment. By contrast, temperate and boreal forests show slight

increases in fragmentation within protected areas, mainly driven by ongoing forestry. These patterns underscore the need for biome-specific conservation strategies that reflect distinct regional pressures.

Although our study provides important insights into global forest fragmentation and its ecological implications, several limitations may affect the accuracy of our estimates. Landsat-derived data likely underestimate fragmentation by failing to detect narrow barriers, such as roads <30 m wide (*48*, *49*). Additionally, this forest cover product does not distinguish between natural forests and agroforestry, potentially underestimating natural forest loss (*37*). Conversely, using a 5-m height threshold to define forests may not fully capture restoration trends, as degraded forests with slow regrowth below this height remain undetected (*37*).

Our study reveals widespread declines in forest ecological integrity over the past two decades, driven largely by human activity. The stark divergence among fragmentation metrics underscores the urgent need for ecologically relevant tools to accurately assess and address these changes. As human pressures on nature intensify, such tools will be essential for guiding effective conservation and reversing global trends in fragmentation and biodiversity loss.

REFERENCES AND NOTES

1. G. B. Bonan, *Science* **320**, 1444–1449 (2008).
2. Y. Pan *et al.*, *Science* **333**, 988–993 (2011).
3. L. Mo *et al.*, *Nature* **624**, 92–101 (2023).
4. H. Ma *et al.*, *Nat. Plants* **9**, 1795–1809 (2023).
5. Y. Zou *et al.*, *Nat. Commun.* **15**, 4658 (2024).
6. Z. Wu *et al.*, *New Phytol.* **240**, 1421–1432 (2023).
7. J. Ma, J. Li, W. Wu, J. Liu, *Nat. Commun.* **14**, 3752 (2023).
8. P. G. Curtis, C. M. Slay, N. L. Harris, A. Tyukavina, M. C. Hansen, *Science* **361**, 1108–1111 (2018).
9. W. F. Laurance, G. B. Williamson, *Conserv. Biol.* **15**, 1529–1535 (2001).
10. A. C. Staver, S. Archibald, S. A. Levin, *Science* **334**, 230–232 (2011).
11. N. M. Haddad *et al.*, *Sci. Adv.* **1**, e1500052 (2015).
12. M. Pfeifer *et al.*, *Nature* **551**, 187–191 (2017).
13. T. Gonçalves-Souza *et al.*, *Nature* **640**, 702–706 (2025).
14. Convention on Biological Diversity, "Aichi Target 11" [United Nations Environment Programe (UNEP), 2010].
15. Intergovernmental Science-Policy Platform on Biodiversity and Ecosystem Services (IPBES), "Kunming-Montreal Global Biodiversity Framework" (UNEP, 2019).
16. L. Fahrig, *Annu. Rev. Ecol. Evol. Syst.* **34**, 487–515 (2003).
17. L. Fahrig, *Glob. Ecol. Biogeogr.* **28**, 33–41 (2019).
18. L. Fahrig *et al.*, *Biol. Conserv.* **230**, 179–186 (2019).
19. R. J. Fletcher Jr. *et al.*, *Biol. Conserv.* **226**, 9–15 (2018).
20. A. E. Martin, L. Fahrig, *Ecology* **99**, 2058–2066 (2018).
21. F. Riva, L. Fahrig, *Conserv. Lett.* **15**, e12881 (2022).
22. J. Rybicki, N. Abrego, O. Ovaskainen, *Ecol. Lett.* **23**, 506–517 (2020).
23. J. N. G. Willmer, T. Püttker, J. A. Prevedello, *Biol. Conserv.* **272**, 109654 (2022).
24. J. Oehri, S. L. R. Wood, E. Touratier, B. Leung, A. Gonzalez, *Biodivers. Conserv.* **33**, 4043–4071 (2024).
25. I. Hanski *et al.*, *Nat. Commun.* **8**, 14504 (2017).
26. M. Beger *et al.*, *Trends Ecol. Evol.* **37**, 1079–1091 (2022).
27. K. S. McGarigal, S. Cushman, M. Neel, E. Ene, FRAGSTATS: Spatial pattern analysis program for categorical maps (2002).
28. N. H. Schumaker, *Ecology* **77**, 1210–1225 (1996).
29. J. A. G. Jaeger, *Landsc. Ecol.* **15**, 115–130 (2000).
30. H. S. He, B. E. DeZonia, D. J. Mladenoff, *Landsc. Ecol.* **15**, 591–601 (2000).
31. I. Hanski, O. Ovaskainen, *Nature* **404**, 755–758 (2000).
32. D. R. Patton, *Wildl. Soc. Bull.* **3**, 171–173 (1975).
33. H. Li, J. Wu, *Landsc. Ecol.* **19**, 389–399 (2004).
34. F. Taubert *et al.*, *Nature* **554**, 519–522 (2018).
35. M. C. Hansen *et al.*, *Sci. Adv.* **6**, eaax8574 (2020).
36. R. Fischer *et al.*, *Sci. Adv.* **7**, eabg7012 (2021).
37. P. Potapov *et al.*, *Front. Remote Sens.* **3**, 856903 (2022).
38. L. Tischendorf, *Landsc. Ecol.* **16**, 235–254 (2001).
39. L. Tischendorf, L. Fahrig, *Oikos* **90**, 7–19 (2000).
40. UNEP-WCMC, IUCN, Protected Planet: The World Database on Protected Areas (WDPA) (2023); www.protectedplanet.net.
41. E. Dinerstein *et al.*, *Bioscience* **67**, 534–545 (2017).
42. J. S. Sze, L. R. Carrasco, D. Childs, D. P. Edwards, *Nat. Sustain.* **5**, 123–130 (2022).
43. J. Geldmann, A. Manica, N. D. Burgess, L. Coad, A. Balmford, *Proc. Natl. Acad. Sci. U.S.A.* **116**, 23209–23215 (2019).
44. P. J. Ferraro, M. M. Hanauer, K. R. E. Sims, *Proc. Natl. Acad. Sci. U.S.A.* **108**, 13913–13918 (2011).
45. V. Graham *et al.*, *Sci. Rep.* **11**, 23760 (2021).
46. P. J. Negret *et al.*, *Conserv. Biol.* **34**, 1452–1462 (2020).
47. J. Geldmann *et al.*, *Biol. Conserv.* **191**, 692–699 (2015).
48. B. Slagter *et al.*, *Remote Sens. Environ.* **315**, 114380 (2024).
49. J. E. Engert *et al.*, *Nature* **629**, 370–375 (2024).
50. Y. Zou, Yibiaozou/Global_ForestFRAG: Global fragmentation trends during 2000-2020. Zenodo (2025); https://doi.org/10.5281/zenodo.14883322.
51. Y. Zou, Global fragmentation trends during 2000-2020. Zenodo (2025); https://doi.org/10.5281/zenodo.15703795.

ACKNOWLEDGMENTS

We thank all the members of the Crowther lab team, including those not listed as coauthors of the study, for their incredible support. **Funding:** This work was supported by grants from the Ambizione Fellowship program (PZ00P3_193646 to C.M.Z.), Bernina Foundation and DOB Ecology (to T.W.C.), Ambizione Fellowship program (PZ00P3_216194 to G.R.S.), and Marie Skłodowska-Curie Actions Postdoctoral Fellowship (EP/Z000831/1 to K.A.G.).
Author contributions: Y.Z., C.M.Z., and T.W.C. conceived, developed, and wrote the paper. Y.Z. performed the analyses. All authors reviewed and provided input on the manuscript.
Competing interests: The authors declare that they have no competing interests. **Data and materials availability:** All data used in this study are from open-source databases and referenced in the paper. Code is available at https://github.com/Yibiaozou/Global_ForestFRAG and Zenodo (*50*). Major dataset and outcome maps of fragmentation metrics are also available at Zenodo (*51*).

SUPPLEMENTARY MATERIALS

science.org/doi/10.1126/science.adr6450
Materials and Methods; Figs. S1 to S23; Tables S1 to S5; References (*52*–*76*); Reproducibility Checklist

Submitted 11 July 2024; resubmitted 19 February 2025; accepted 14 July 2025
10.1126/science.adr6450